Generalized TLM Block Meshing Scheme Based on N-port Network Representation

Abdelrahman Ijjeh, Marylene Cueille, Jean-Lou Dubard, Michel Ney

Generalized TLM Block Meshing Scheme Based on N-port Network Representation

A. Ijjeh [(1)], M. Cueille [(1)], J-L. Dubard [(1)] and M. M. Ney [(2)]

(1) Université Côte d'Azur, CNRS, LEAT, 06903 Sophia Antipolis, France
(2) IMT Atlantique, Lab-STICC, CS 83818, 29238 Brest Cedex 3, France

***Abstract* — This article revisits the ideal transformer model used at the interface between different sub-grids in non-structured TLM meshes. The derivation of the voltage-exchange equations between two subdomains with an arbitrary meshing ratio and connection topology is presented. The voltage-exchange process is then generalized as a scattering-matrix of an N-port network that processes all desired properties for a perfect interface. This S-matrix is derived directly for its properties and no concrete physical representation is required. Moreover, the necessary conditions that ensure stability of such connection will be presented in the final submission.**

***Index Terms* — Block meshing, C-matrix, N-port network, S-matrix, time-domain methods, Transmission-Line Matrix method.**

I. Introduction

Meshing per blocks in the Transmission-Line Matrix (TLM) method is a powerful discretization scheme to handle multiscale electromagnetic (EM) problems [1] [2]. This technique allows for adequate geometrical representation of the fine details locally, without exhausting the computational resources [3]. Moreover, the scheme based on the ideal transformer was shown to be stable, lossless and accurate when a global time-step (Δt) is used. The latter corresponds to the smallest CFL limit in the entire computational domain (usually inside the fine region). However, even with a global time-step this meshing scheme can expedite the TLM simulations many-folds as compared to uniform fine-meshing or structured irregular-meshing schemes.

In the original work of [1], two connection topologies were proposed namely, the current-based and the voltage-based connections. The later was shown to be unstable when fields rapidly change inside the fine grid (e.g., a punctual current source in the fine grid) [3]. The ideal transformer model works equally for SCN or HSCN based TLM nodes. However, and without loss of generality, we consider only cubic SCN nodes in this article [3]. Note that the SCN node has some very attractive features as compared to other ones. For instance, the characteristic impedance of the arms is always the one of the free-space ($120\pi\ \Omega$). Moreover, media presence is taken into consideration at cell centers via stubs [2] in simple media, or filtering process for general linear media. Furthermore, the analogy between the TLM and circuit theory and the previously mentioned two features, allows one to model lumped elements in a straightforward manner.

The objective of this article is three-folds, firstly, to present a methodology to derive the voltage-exchanges equations for a generalized/arbitrary connection topology. Secondly, to model the voltage-exchanges as N-port network with an S-matrix that processes all desired features. Finally, to investigate the necessary conditions that guarantee stability when global time-step is used.

II. Mathematical Model

Consider a computational domain discretized by using block meshing (Cartesian non-conformal local refinement). The interface between to sub-grids is shown in fig. 1.

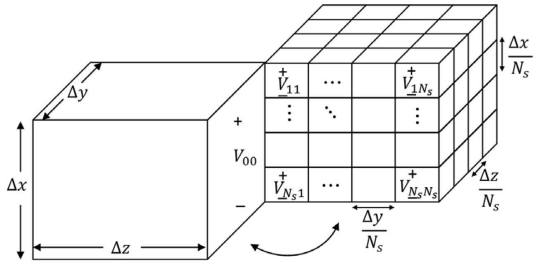

Fig. 1. The physical interface between a coarse and a fine subdomains (one large cells is adjacent to N_s^2 small cells).

Any voltage/current signal in the TLM mesh (including interfaces) can be decomposed into incident $V_{i,j}^{inc}$ and reflected $V_{i,j}^{ref}$ voltages [2]:

$$V_{i,j} = V_{i,j}^{inc} + V_{i,j}^{ref} \tag{1.a}$$

$$I_{i,j} = \frac{1}{Z_0}\left(V_{i,j}^{inc} - V_{i,j}^{ref}\right) \tag{1.b}$$

where Z_0 is the free-space characteristic impedance.

A. Current-Based Connection Topology

As a starting point, we consider the connection topology shown in fig.2, namely, the current-based topology [1]. By applying the KCL, KVL Kirchhoff's laws and (1), one obtains a linear system involving reflected and incident voltages. After some mathematical manipulations, one can obtain the voltages exchange model [1]:

$$V_{i,j}^{ref} = (I_i - I)\frac{Z_i}{f_{ij}} - V_{i,j}^{inc} \tag{2}$$

Different terms used in (2) are defined in table I.

TABLE I

DEFINITIONS OF TERMS USED IN (2) [1]

$f_{ij}=\frac{\Delta x_{ij}}{\Delta y_{ij}}$	$f_{00}=-\frac{\Delta x_{00}}{\Delta y_{00}}$	$Y_{ij}=\frac{1}{Z_0}$
$Z_i=\frac{1}{\sum_j Y_{ij}/f_{ij}{}^2}$	$I_i=2\sum_j \frac{Y_{ij}V_{i,j}^{inc}}{f_{ij}}$	$I=\frac{\sum_i Z_i I_i}{\sum_i Z_i}$

In table I, the summations over i-index are for $i=\{0,1,2,\cdots,N_s\}$. The summations over j-index are for $=\{1,2,\cdots,N_s\}\ \forall\, i>0$, and consist of one element $j=0$ when $i=0$.

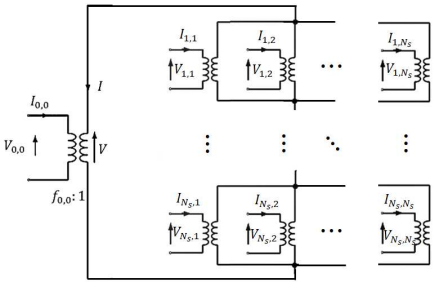

Fig. 2. Schematic diagram for the current-based voltages-exchange topology [1].

Model (2) can be expressed in a more compact form as [4][5]:

$$\bar{V}^{ref}=\bar{\bar{\Lambda}}\bar{V}^{inc} \tag{3}$$

where $\bar{V}^{ref}$ is the vector of reflected voltages from the interface:

$$\bar{V}^{ref}=\left[V_{0,0}^{ref},V_{1,1}^{ref},V_{1,2}^{ref},\cdots V_{N_s,N_s}^{ref}\right]^T \tag{4.a}$$

For simplicity, this vector can be indexed as:

$$\bar{V}^{ref}=\left[V_1^{ref},V_2^{ref},V_3^{ref},\cdots V_{N_p}^{ref}\right]^T \tag{4.b}$$

where the N_p number of ports ${N_s}^2+1$, and T is the matrix transpose operator. Similarly for the incident voltage vector:

$$\bar{V}^{inc}=\left[V_1^{inc},V_2^{inc},V_3^{inc},\cdots V_{N_p}^{inc}\right]^T \tag{4.c}$$

The Scattering matrix $\bar{\bar{\Lambda}}$ is a square matrix of size (N_s^2+1) defined as:

$$\bar{\bar{\Lambda}}=\bar{\bar{A}}-\bar{\bar{I}}_{N_p} \tag{5.a}$$

$\bar{\bar{I}}_{N_p}$ is the identity matrix of size N_p and the matrix $\bar{\bar{A}}$ is defined as:

$$\bar{\bar{A}}_{ij}=\begin{cases}0, & if \quad i=j=1\\ \frac{1}{N_s}, & if \quad j=1, \quad 2\le i\le N_p\\ \frac{1}{N_s}, & if \quad i=1, \quad 2\le j\le N_p\\ -\left(\frac{1}{N_s}\right)^2+\frac{2}{N_s}, & if \quad \left\lfloor\frac{i-2}{N_s}\right\rfloor=\left\lfloor\frac{j-2}{N_s}\right\rfloor, 2\le j,i\le N_p\\ -\left(\frac{1}{N_s}\right)^2, & if \quad \left\lfloor\frac{i-2}{N_s}\right\rfloor\ne\left\lfloor\frac{j-2}{N_s}\right\rfloor, 2\le j,i\le N_p\end{cases} \tag{5.b}$$

where $\lfloor\cdot\rfloor$ is the largest integer (floor) operator.

B. *Voltage-Based Connection Topology*

Similarly, the voltage-based connection topology is shown in fig.3 below;

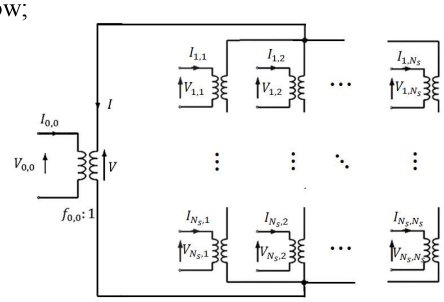

Fig. 3. Schematic diagram for the voltage-based voltages-exchange topology [1].

One can obtain the corresponding scattering matrix $\bar{\bar{\Lambda}}$ for the connection in fig.3 as:

$$\bar{\bar{\Lambda}}=\bar{\bar{A}}+\bar{\bar{I}}_{N_p} \tag{6.a}$$

where the matrix $\bar{\bar{A}}$ is defined as:

$$\bar{\bar{A}}_{ij}=\begin{cases}0, & if \quad i=j=1\\ \frac{1}{N_s}, & if \quad j=1, \quad 2\le i\le N_p\\ \frac{1}{N_s}, & if \quad i=1, \quad 2\le j\le N_p\\ \left(\frac{1}{N_s}\right)^2-\frac{2}{N_s}, & if \quad \left\lfloor\frac{i-2}{N_s}\right\rfloor=\left\lfloor\frac{j-2}{N_s}\right\rfloor, 2\le j,i\le N_p\\ \left(\frac{1}{N_s}\right)^2, & if \quad \left\lfloor\frac{i-2}{N_s}\right\rfloor\ne\left\lfloor\frac{j-2}{N_s}\right\rfloor, 2\le j,i\le N_p\end{cases} \tag{6.b}$$

In both (5) and (6) one can notice that the scattering matrices are not matched (diagonal elements are not zeros).

C. *Generalized Voltage-Exchange Scattering-Matrix*

Consider the generic N_p-port network shown in fig.4. Again, as in (3), the voltage-exchanges are governed by a scattering matrix $\bar{\bar{\Lambda}}$.

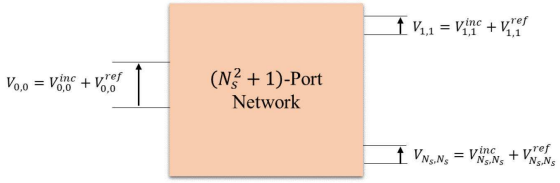

Fig. 4. The interface between two subdomains with a subgridding ratio N_s as N_p-port network.

An ideal matrix $\bar{\bar{\Lambda}}$ for our purpose should have the following features [4]-[7]:

I. *Lossless property*

The scattering matrix $\bar{\bar{\Lambda}}$ should be unitary:

$$\bar{\bar{\Lambda}}\,\bar{\bar{\Lambda}}^H=\bar{\bar{I}}_{N_p} \tag{7.a}$$

where H is the matrix Hermitian operator. Note that since $\overline{\overline{\Lambda}}$ is a real matrix, its transpose is equivalent to its Hermitian. Furthermore, if $\overline{\overline{\Lambda}}$ fulfills (7.a) then all its eigenvalues are on the unit circle.

II. Matched network

To guarantee reflection-less ports, elements on the main diagonal of the scattering matrix $\overline{\overline{\Lambda}}$ should equal to zero.

$$\overline{\overline{\Lambda}}_{ii} = 0 \tag{7.b}$$

III. Reciprocal

Reciprocity, can be viewed mathematically as the symmetry of the matrix $\overline{\overline{\Lambda}}$.

$$\overline{\overline{\Lambda}} = \overline{\overline{\Lambda}}^{T} \tag{7.c}$$

IV. Power divider/combiner

Signal coming at port 1 is equally divided into the remaining $N_p - 1$ ports, while signals coming through ports $\{2\ to\ N_p\}$ are combined at port 1.

$$\overline{\overline{\Lambda}}_{1j} = \frac{1}{N_s}, \qquad \forall\ 2 \le j \le N_p \tag{7.d}$$

$$\overline{\overline{\Lambda}}_{i1} = \frac{1}{N_s}, \qquad \forall\ 2 \le i \le N_p \tag{7.e}$$

The objective is to build a scattering matrix $\overline{\overline{\Lambda}}$ that has all characteristics (7). Finding a general solution for all possible $\overline{\overline{\Lambda}}$ and for any subgridding ratio N_s might be outside the scope of this study. However, in literature one finds a family of matrices -known as the C-matrices- that fulfills (7), as shown in fig.5.

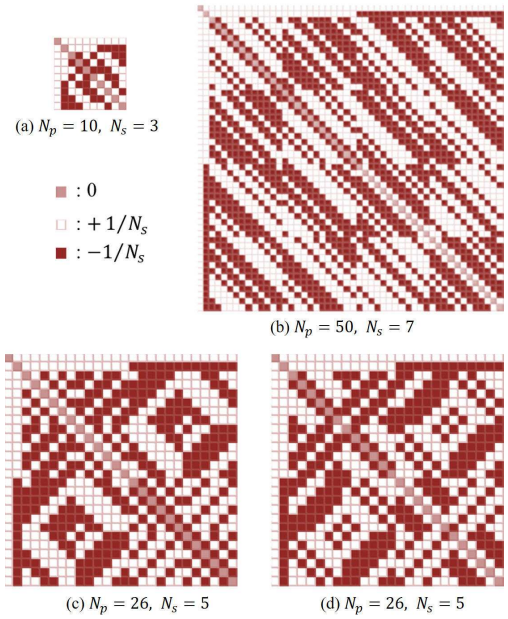

Fig. 5. (a) C-matrix of size 10, (b) C-matrix of size 50, (c) first solution for the C-matrix 26, (d) second solution of C-matrix 26.

These matrices come with specific sizes (e.g., 6, 10, 26, 50 …etc.). Only some sizes fit our requirements, for instance $N_p = 10 = 3^2 + 1$ (for $N_s = 3$), and $N_p = 50 = 7^2 + 1$ (for $N_s = 7$). Fig. 5a and fig. 5b show the structure of this matrix for the cases $N_p = 10$ and $N_p = 50$. In fig. 5c and fig. 5d, two different solutions for the C-matrix for the case $N_p = 26 = 5^2 + 1$ (for $N_s = 5$) are displayed. Note that, C-matrices belong to a more general family of matrices known as the Weighing Matrices. A C-matrix of size n is a W-matrix $(n, n-1)$ [8].

An ideal C-matrix represents a lossless and matched network; signal entering any port will split among other ports with no reflections. To avoid any dissipation losses within the system, the network must contain ideal transformers only and no resistances. Moreover, since the C-matrix is real, no inductors or capacitors can exist in the corresponding network.

III. Results and Discussions

In this section, we discuss two experiments; firstly, we study the properties of the scattering matrix $\overline{\overline{\Lambda}}$. Then, we implement it in the TLM algorithm to test its performance.

A. Eigenvalues Distribution of the Voltages-Exchange $\bar{\bar{\Lambda}}$ Matrix (case Ns=3)

For instance, the scattering matrix (C-matrix of size 10) that fulfills the conditions (7), (see fig.5a) is:

$$\bar{\bar{\Lambda}} = \frac{1}{3}\begin{pmatrix} 0 & 1 & 1 & 1 & 1 & 1 & 1 & 1 & 1 & 1 \\ 1 & 0 & 1 & 1 & 1 & 1 & -1 & -1 & -1 & -1 \\ 1 & 1 & 0 & -1 & 1 & -1 & 1 & 1 & -1 & -1 \\ 1 & 1 & -1 & 0 & -1 & 1 & -1 & 1 & 1 & -1 \\ 1 & 1 & 1 & -1 & 0 & -1 & -1 & -1 & 1 & 1 \\ 1 & 1 & -1 & 1 & -1 & 0 & 1 & -1 & -1 & 1 \\ 1 & -1 & 1 & -1 & -1 & 1 & 0 & 1 & -1 & 1 \\ 1 & -1 & 1 & 1 & -1 & -1 & 1 & 0 & 1 & -1 \\ 1 & -1 & -1 & 1 & 1 & -1 & -1 & 1 & 0 & 1 \\ 1 & -1 & -1 & -1 & 1 & 1 & 1 & -1 & 1 & 0 \end{pmatrix}$$

The eigenvalues of $\bar{\bar{\Lambda}}$ are $\lambda_i = -1$ for $1 \le i \le 5$, and $\lambda_i = +1$ for $6 \le i \le 10$.

For comparison, the $\overline{\overline{\Lambda}}$ matrix corresponding to the current-based connection topology (5) is:

$$\bar{\bar{\Lambda}} = \frac{1}{9}\begin{pmatrix} 0 & 3 & 3 & 3 & 3 & 3 & 3 & 3 & 3 & 3 \\ 3 & -4 & 5 & 5 & -1 & -1 & -1 & -1 & -1 & -1 \\ 3 & 5 & -4 & 5 & -1 & -1 & -1 & -1 & -1 & -1 \\ 3 & 5 & 5 & -4 & -1 & 1 & -1 & -1 & -1 & -1 \\ 3 & -1 & -1 & -1 & -4 & 5 & 5 & -1 & -1 & -1 \\ 3 & -1 & -1 & -1 & 5 & -4 & 5 & -1 & -1 & -1 \\ 3 & -1 & -1 & -1 & 5 & 5 & -4 & 1 & -1 & -1 \\ 3 & -1 & -1 & -1 & -1 & -1 & 1 & -4 & 5 & 5 \\ 3 & -1 & -1 & -1 & -1 & -1 & -1 & 5 & -4 & 5 \\ 3 & -1 & -1 & -1 & -1 & -1 & -1 & 5 & 5 & -4 \end{pmatrix}$$

One can observe that the matrix is not matched; however, it is lossless and is eigenvalues are $\lambda_i = -1$ for $1 \le i \le 7$, and $\lambda_i = +1$ for $8 \le i \le 10$.

Finally, the $\overline{\overline{\Lambda}}$ matrix corresponding to the voltage-based connection topology (6) is:

$$\bar{\bar{\Lambda}} = \frac{1}{9}\begin{pmatrix} 0 & 3 & 3 & 3 & 3 & 3 & 3 & 3 & 3 & 3 \\ 3 & 4 & -5 & -5 & 1 & 1 & 1 & 1 & 1 & 1 \\ 3 & -5 & 4 & -5 & 1 & 1 & 1 & 1 & 1 & 1 \\ 3 & -5 & -5 & 4 & 1 & 1 & 1 & 1 & 1 & 1 \\ 3 & 1 & 1 & 1 & 4 & -5 & -5 & 1 & 1 & 1 \\ 3 & 1 & 1 & 1 & -5 & 4 & -5 & 1 & 1 & 1 \\ 3 & 1 & 1 & 1 & -5 & -5 & 4 & 1 & 1 & 1 \\ 3 & 1 & 1 & 1 & 1 & 1 & 1 & 4 & -5 & -5 \\ 3 & 1 & 1 & 1 & 1 & 1 & 1 & -5 & 4 & -5 \\ 3 & 1 & 1 & 1 & 1 & 1 & 1 & -5 & -5 & 4 \end{pmatrix}$$

Again, one can notice that this matrix is not matched; however, it is lossless and is eigenvalues are $\lambda_i = -1$ for $1 \leq i \leq 3$, and $\lambda_i = +1$ for $4 \leq i \leq 10$.

B. Fundamental Resonant Mode in a Rectangular Cavity

The air-filled cubic cavity (shown in fig.6) is excited by a narrow band modulated Gaussian-pulse centered on the fundamental resonant frequency ($f_0 = 10.61$ GHz). Perfect Electric Conducting (PEC) walls cover the cavity. Its top half is discretized into cubic cells 4 mm of mesh-size, the bottom half is discretized into cubic cells of $\Delta x = 1.333$ mm. the subgridding ratio $N_s = 3$. In this experiment, we use the scattering matrices shown in the previous experiment to model the voltage-exchange between both two subdomains. The goal is to test for stability for the different scattering matrices, as well as the accuracy of results.

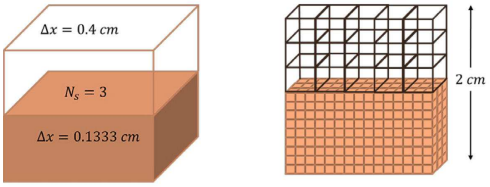

Fig. 6. (a) air-filled cubic cavity of side length 2 cm discretized using block meshing (Ns=3), (b) cross section of the cavity (frontal plane).

In fig.7, the fields' distributions for different fields' components of the fundamental TE resonant mode are shown for the different connection schemes. The error in computing the resonant frequency of this mode for the three schemes was less than 1.0%. Moreover, simulations were stable for the different connection schemes for 500 thousands iterations, with no sign of instability observed.

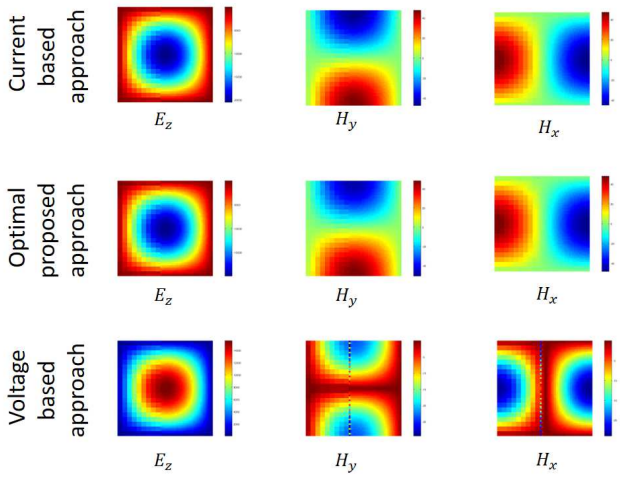

Fig. 7, fields' distributions for the dominant transverse electric mode, interface using three approaches mentioned in example A.

VI. Conclusion

This article, presents an alternative approach to derive the scattering matrix that governs the voltage exchange in non-conformal TLM meshing. No specific concrete physical model (e.g., ideal transformer) at the interface between coarse and fine cells is required.

Acknowledgement

This work benefited from access to CINES computing resources through the 2021 A0100505122 resource allocation attributed by GENCI.

References

[1] J. Wlodarczyk, "New multigrid interface for the TLM method", Electron. Lett., vol. 32, no. 12, pp. 1111-1112, 1996.

[2] P. B. Johns, "A symmetrical condensed node for the TLM method", IEEE Trans. Microw. Theory Techn., vol. MTT-35, no. 4, pp. 370-377, 1987.

[3] A. A. Ijjeh, M. Cueille, J. -L. Dubard and M. M. Ney, "Dispersion and Stability Analysis for TLM Unstructured Block Meshing," in IEEE Transactions on Microwave Theory and Techniques, vol. 69, no. 10, pp. 4352-4365, Oct. 2021.

[4] H. Carlin. (1956). The scattering matrix in network theory. IRE Transactions on Circuit Theory, 3(2), 88-97.

[5] K. Kurokawa, "Power Waves and the Scattering Matrix," in IEEE Transactions on Microwave Theory and Techniques, vol. 13, no. 2, pp. 194-202, March 1965, doi: 10.1109/TMTT.1965.1125964.

[6] V. Belevitch, Classical Network Theory, San Francisco: Holden-Day, 1968.

[7] V. Belevitch V (1950). "Theory of 2n-terminal networks with applications to conference telephony". Electrical Communication. 27: 231–244.

[8] C. J. Colbourn, CRC handbook of combinatorial designs. CRC press, 2010.

[9] D. M. Pozar, Microwave engineering. Hoboken, NJ:Wiley, pp. 300-350, 2012.